Available online at www.sciencedirect.com
ScienceDirect
Estuarine, Coastal and Shelf Science 72 (2007) 235–246
ESTUARINE COASTAL AND SHELF SCIENCE
www.elsevier.com/locate/ecss

Observations of tidal and springtime sediment transport in the upper Delaware Estuary

Timothy L. Cook [a,1], Christopher K. Sommerfield [a,*], Kuo-Chuin Wong [b]

[a] College of Marine and Earth Studies, University of Delaware, 210 Cannon Marine Studies Lab, Lewes, DE 19958, USA
[b] College of Marine Studies, University of Delaware, Newark, DE 19716, USA

Received 23 January 2006; accepted 19 October 2006
Available online 8 December 2006

Abstract

Suspended-sediment transport in the upper Delaware Estuary was investigated in Spring 2003 to examine mechanisms of material exchange from the tidal river to the turbidity maximum zone in the lower estuary. Timeseries records of currents and suspended-sediment concentration (SSC) were obtained between 18 March and 10 June 2003 using moored instrumentation deployed at two locations spanning the tidal river–estuary transition: (1) Tinicum Island, 90 km up-estuary of the Delaware Bay mouth in tidal freshwater; and (2) New Castle Flats, 40 km down-estuary of Tinicum in oligohaline waters. Environmental conditions during the observational period were typical for the spring season and included two river peakflows (1000–2000 $m^3\ s^{-1}$) and several moderate remote-wind events. Results indicate that SSC and tidal sediment flux vary spatially in the estuary with local current magnitude and the proximity of patches of easily resuspendable sediment. Landward of the turbidity maximum zone, SSC was not correlated with current velocity due to depletion of bed sediment sources early in the tidal cycle. In contrast, SSC and velocity within the turbidity maximum zone were well correlated due to an abundance of fine sediment generated by resuspension and advection. At both observational sites the depth-averaged residual current (Eulerian mean) and net sediment flux were seaward, and the flux magnitude increased 3–4 fold during river peakflow events on account of elevated ebb flow and bottom scour. The seaward residual current, mostly compensatory flow for Stokes Drift on flood tide, is an important mechanism of sediment transport to the estuarine turbidity maximum zone. Averaged over the 80-day study period, the cross-sectionally averaged sediment flux past New Castle ($11 \pm 4 \times 10^8$ kg) was significantly larger than that at Tinicum ($4 \pm 1 \times 10^8$ kg), and twofold larger than the estimated influx from river tributaries ($5 \pm 1 \times 10^8$ kg). The mass imbalance ($\sim 7 \times 10^8$ kg) suggests that eroded bed sediment, previously deposited and stored in the upper estuary, was a major source of material to the turbidity maximum zone in Spring 2003.

Keywords: tidal currents; sediment transport; estuarine sedimentation; sediment budget; Delaware River

1. Introduction

As in many urbanized estuaries worldwide, fine-grained sediment is central to a number of issues in the Delaware Estuary including shoaling of shipping channels, dispersal of particle-borne contaminants, and primary productivity. The Delaware Estuary supports one of the world's largest freshwater ports, the Philadelphia–Wilmington complex, which in the United States is second to only New York Harbor in terms of ship traffic. The estuary also sustains one of the longest continuous coastal marsh systems on the U.S. Mid-Atlantic coast, and evidence of accelerated erosion has raised concerns over the sustainability of the marsh in the face of rising sea level (Kraft et al., 1992; Kearney et al., 2002). Vigorous maintenance dredging in the upper estuary permanently removes a significant quantity of muddy sediment that would otherwise disperse seaward to lower estuary and marsh environments; hence, human intervention has disturbed the natural throughput of sediment from sources to sinks.

The general circulation of the Delaware Estuary is rather well known (Pape and Garvine, 1982; Wong and Garvine,

* Corresponding author.
E-mail address: cs@udel.edu (C.K. Sommerfield).
[1] Present address: Department of Geosciences, University of Massachusetts, 611 North Pleasant Street, Amherst, MA 01003, USA.

0272-7714/$ - see front matter © 2007 Elsevier Ltd. All rights reserved.
doi:10.1016/j.ecss.2006.10.014

1984; Galperin and Mellor, 1990; Garvine et al., 1992; Münchow et al., 1992; Wong and Moses-Hall, 1998; Janzen and Wong, 2002), but the sedimentary system is poorly understood by comparison. Specifically, mechanisms and rates of sediment mass transport from the tidal Delaware River to sites of burial in the estuary, marsh and bay are unknown. Thus, there is a pressing need to determine the relative influences of tidal and subtidal (fluctuations longer than a tidal period) currents, gravitational circulation, and particle dynamics—flocculation, deposition and resuspension—on net sediment flux in the system (e.g., Uncles et al., 1994; Geyer et al., 2001). With this need in mind, this study aimed to characterize transport conditions at the transition between the tidal river and estuary using timeseries measurements of currents and suspended-sediment concentration. The specific objectives were to (1) document tidal and subtidal variations in sediment transport during the spring season, when most of the annual sediment load is delivered by the river tributaries, and (2) elucidate the mechanisms that maintain the turbidity maximum zone at its landward extent. Significantly, this contribution represents the first quantitative study of suspended-sediment transport in the upper Delaware Estuary.

2. Regional background

The tidal Delaware River, estuary and bay (Delaware Estuary hereafter) is the second largest estuarine system on the U.S. Atlantic coast, stretching 215 km from the bay mouth to the head-of-tides at Trenton, New Jersey (Fig. 1). The estuary is classified as weakly stratified to well-mixed on account of the large tidal discharge at the bay mouth (1.5×10^5 m^3 s^{-1}) relative to the mean influx of freshwater (650 m^3 s^{-1}; Garvine et al., 1992). The upper estuary is perennially well-mixed with salinities ranging from 0 to 5 (Practical Salinity Scale), increasing seaward in the lower estuary to the bay to a maximum of 25–30. The estuary displays transient stratification which tends to be strongest ($\delta_s = 3$–5) at the transition between the lower estuary and bay, especially following springtime freshwater pulses known as "freshets" (Sharp et al., 1986). The Delaware River at Trenton contributes over 60% of the total freshwater input to the estuary and has a mean annual discharge of 330 m^3 s^{-1}; monthly mean discharge of the Delaware is highest and lowest in April and September, respectively (Fig. 2). Peakflow typically reaches 1500–2000 m^3 s^{-1} on an annual basis and exceeds 5000 m^3 s^{-1} on a recurrence interval of 20 years. The Schuylkill and Christina rivers are respectively the second and third largest tributaries with mean annual discharges of 77 and 19 m^3 s^{-1}.

On average, a total of 1.3×10^9 kg year^{-1} of suspended sediment is delivered to the Delaware Estuary by river tributaries (Mansue and Commings, 1974; Walsh, 2004). The Delaware River mainstem usually accounts for 50% of the total influx, the Schuylkill and Christina rivers contribute 20% and 8%, respectively, whereas the remaining 22% is supplied by numerous coastal plain streams (Mansue and Commings, 1974). A large fraction of the total annual influx of sediment occurs during the months of March and April in association with freshet events (Fig. 2). The suspended-sediment concentration (SSC) in surface waters of the estuary is typically 10–100 mg L^{-1}, and is highest within estuarine turbidity

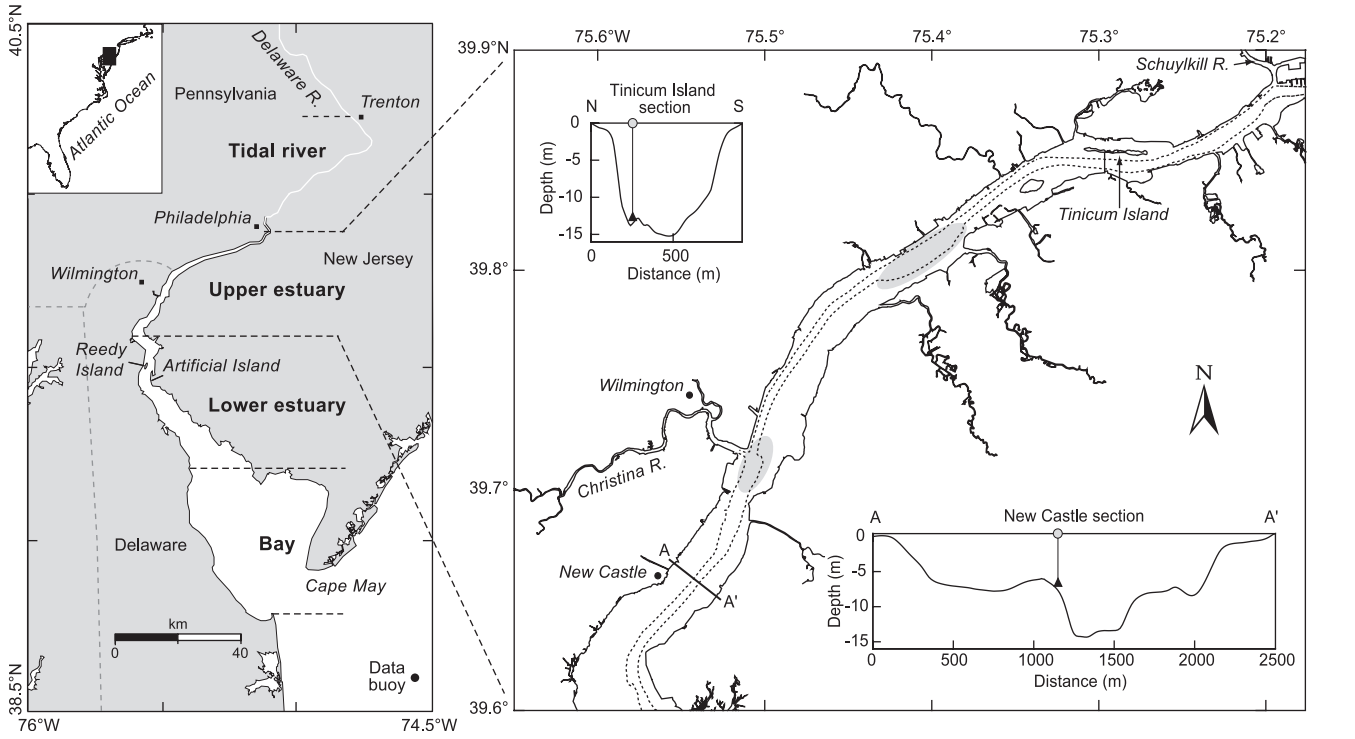

Fig. 1. (Left) Map of the tidal Delaware River, estuary and bay with geographic features referred to in the text. (Right) Segment of the upper estuary showing the locations of moored sensors and cross-sectional bathymetry. The dashed line denotes to 10 m isobath, which outlines the main shipping channel. Shaded areas depict mud depositional zones identified by Sommerfield and Madsen (2004) and referred to in the text.

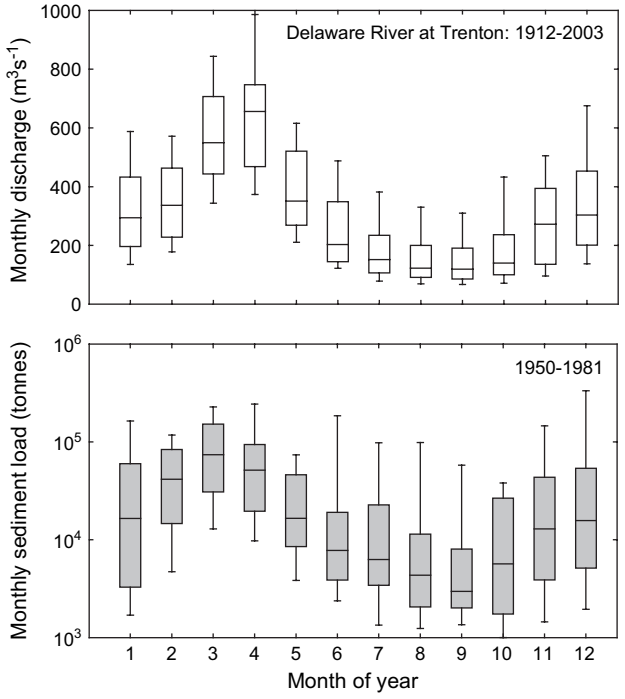

Fig. 2. Box-and-whisker plots of mean monthly water discharge (top) and suspended-sediment load (bottom) for the Delaware River at Trenton from measurements by the U.S. Geological Survey. Bottom, middle and top lines of each box correspond to 25th, 50th and 75th percentiles, respectively, and bottom and top lines of the whiskers are respectively the 10th and 90th percentiles.

maximum zone (ETM), which extends 50–120 km from the bay mouth (Biggs et al., 1983). The landward limit of the ETM generally falls within 0.1–1 salinity waters, whereas the high-concentration core is often present in the vicinity of Artificial Island. In addition to SSC, the mean size of suspended particle aggregates (flocs) increases from the tidal river to the ETM zone, and decreases from the lower estuary to bay (Gibbs et al., 1983).

Tides in the estuary are dominated by the M_2 constituent with a mean range of 1.3 m at the mouth of Delaware Bay, increasing to 2.7 m at the head-of-tides (Parker, 1991). The oceanic tide becomes distorted starting about 130 km landward of the mouth due to friction and the strongly convergent geometry of the basin. Slackwater in the upper estuary occurs ~1–1.5 h after high or low water. Maximum surface currents at spring tide range from 1.5 m s^{-1} in narrow segments of the tidal river and upper estuary, decreasing to 0.75 m s^{-1} in the lower estuary and bay.

The area targeted for study is a 40-km segment of the upper estuary between New Castle, Delaware, and Tinicum Island, Pennsylvania (Fig. 1). Here the estuary is typically oligohaline but transitions to tidal freshwater during periods of high river discharge. The channel is 1–2.5 km wide and has a maximum depth of 15 m in the axial shipping channel (deepened from a natural depth of 7–9 m). The bottom type is highly heterogeneous and includes Pleistocene fluvial sand and gravel, Holocene–modern estuarine mud, and bedrock exposures (Biggs and Beasley, 1988). Mud accumulation in the upper estuary is patchy and tends to be centered in the shipping channel (Sommerfield and Madsen, 2004). Maintenance dredging is frequent to counter intense deposition, but there were no dredging operations in the study area for at least 1 year prior to the observational period.

3. Methods

The field experiment consisted of an 80-day instrument deployment from 18 March to 10 June 2003, as well as two hydrographic surveys of water properties conducted aboard the RV *Cape Henlopen* in conjunction with mooring deployment and recovery cruises. Identically instrumented moorings were deployed at New Castle (39°39.28′ N, 75°32.93′ W) and Tinicum Island (39°51.03′ N, 75°17.92′ W) just adjacent to the shipping channel in 9 m and 15 m water depths, respectively (Fig. 1). The bottom type at the Tinicum Island site is silty sand, and is clayey silt at the New Castle site (Table 1). Water-column currents at both sites were measured using an upward-looking 600-kHz acoustic Doppler current profiler (ADCP, RD Instruments) configured for a 0.5-m bin size. The ADCP was mounted 2 m and 3 m above the bottom at Tinicum Island and New Castle, respectively. Additionally, point velocity was measured at 0.9 m (Tinicum Island) and 0.5 m (New Castle) above the bottom using a 5-MHz acoustic Doppler velocimeter (ADV, Sontek Hydra-Ocean Probe). At both sites, optical backscatter (D&A Instruments OBS-3 sensor) was recorded at two points in the water column: (1) near the elevation of the ADV probe; and (2) 5 m below the water surface. Tidal height was computed from pressure data recorded by the ADCP and ADV units. All sensors were configured for a sampling scheme consisting of 150-s bursts at 1-Hz sampling rate every 15 min.

Axial sections of temperature, salinity and SSC were constructed from CTD and optical backscatter profiles collected

Table 1
Summary of timeseries measurements in the upper Delaware Estuary. Depth-averaged current ($\langle U_{mean} \rangle$) and suspended-sediment concentration (SSC) data are flood- and ebb-period averages for all spring and neap tides

Property	New Castle		Tinicum Island	
	Spring	Neap	Spring	Neap
Tidal range (m)	1.85	1.55	1.80	1.60
h (average water depth, m)	9.15	9.20	15.10	15.20
$\langle U_{mean} \rangle$ (flood, cm s^{-1})[a]	60	50	80	70
$\langle U_{mean} \rangle$ (ebb, cm s^{-1})	95	85	90	85
SSC_{max} (flood, bottom, mg L^{-1})[a]	650	450	90	110
SSC_{max} (ebb, bottom, mg L^{-1})	775	525	140	155
SSC_{min} (slack, bottom, mg L^{-1})	85	65	45	45
SSC_{max} (flood, mid depth, mg L^{-1})	165	120	40	40
SSC_{max} (ebb, mid depth, mg L^{-1})	160	115	50	40
SSC_{min} (slack, mid depth, mg L^{-1})	30	30	20	20
d_{50} (median grain size, mm)	0.012		1.0	
z_0 (cm, from Soulsby, 1983)	0.02		0.03	
W_s (bulk settling velocity, cm s^{-1})	0.40 ± 0.23		0.18 ± 0.13	
U_{cr} (erosion velocity, cm s^{-1})	30 ± 8		30 ± 7	

[a] Bottom and mid-depth SSC data are from the bottom-mounted and moored OBS sensors, respectively.

during the hydrographic surveys. Measurements were made with a Seabird SeaCat SBE 25 CTD with an integrated OBS-3 sensor at 16 stations spaced regularly between Delaware Bay mouth and Tinicum Island. Water samples were collected on each CTD cast using a 1.8-L Nisken bottle triggered 0.5 m above the bottom. The OBS-3 sensors (moored and shipboard) were calibrated against filtered water samples following methods described in Kineke and Sternberg (1992). In all cases OBS voltage and SSC were strongly correlated ($r^2 \geq 0.99$), and a robust regression equation was obtained. Details of OBS-3 sensor calibrations are provided in Cook (2004).

Ancillary hydrological and meteorological data were obtained from the U.S. Geological Survey (USGS) and National Oceanic and Atmospheric Administration (NOAA) databases. USGS stream gauging stations provided daily river discharge for the Delaware at Trenton and other major tributaries. Daily sediment loads for the Delaware, Schuylkill, and Christina rivers were estimated from suspended-sediment rating curves developed from archived USGS sediment concentration and water discharge data (USGS, 2005), and following methods described in Syvitski et al. (2000). Hourly wind direction and velocity data were obtained from National Data Buoy Center (NDBC) for Station 44009 (see Fig. 1 for location).

4. Results and interpretation

4.1. Regional salinity and SSC distribution

A freshet occurred in late March, one week after the deployment of sensors, and a second event occurred one week prior to recovery in early June (Fig. 3). The combined discharge of the Delaware and Schuylkill rivers reached $\sim$2500 m^3 s^{-1} during the first freshet, whereas the second event was somewhat lower at 1700 m^3 s^{-1}. Although salinity was not measured at the mooring sites, a USGS sensor located 30 km down-estuary of the study area (at Reedy Island) recorded salinities ranging from 0.1 to 4 during the deployment period (Fig. 3). The record shows that the freshet pulses displaced the salt intrusion to the lower estuary for a period of about two weeks.

Hydrographic sections for the 18 March (spring tide, ebb) and 10 June 2003 (neap tide, ebb) surveys display longitudinal gradients of salinity and SSC typical for Delaware Estuary—a vertically mixed upper estuary and a weakly stratified lower estuary and bay (Fig. 4). During both surveys the ETM extended roughly 60–120 km landward of the bay mouth; the high-concentration core was present up-estuary of the salt front, whereas the landward limit broadly coincided with salt intrusion. In June the ETM core was observed $\sim$20 km down-estuary of its March location and contained a much larger quantity of suspended sediment. Also in June, a secondary SSC maximum was present landward of the primary ETM. More sediment was present in the water column during the neap-tide survey than during the spring-tide survey, contrary to the typical spring–neap trend in river-estuaries (e.g., Allen et al., 1980). As elaborated later, the observed changes in ETM locus and sediment mass are most likely related to riverflow variability during the observational period.

4.2. Tidal variation in currents and SSC

Profiles of current velocity and SSC averaged over all floods and ebbs at spring and neap tides are shown in Fig. 5. These composite profiles of velocity were constructed by fitting a logarithmic curve to synoptic ADCP and ADV data to estimate velocity between the ADV (<1 m above bottom) and the lowest ADCP bin ($\leq$3 m above bottom), as well as from the highest bin to the water surface. The timeseries of near-bottom and mid-water SSC were used to model SSC profiles for the entire water column using the analytical solution of the Rouse equation (Orton and Kineke, 2001). Shear velocity (u_*) was estimated using the well-known von Karman–Prandtl equation and published roughness length (z_0) values representative of bed properties at the measurement sites (Soulsby, 1983). Parameters used to construct velocity and SSC profiles are presented in Table 1.

The shape of the velocity envelope was similar during spring and neap periods—the bottom-boundary layer extended

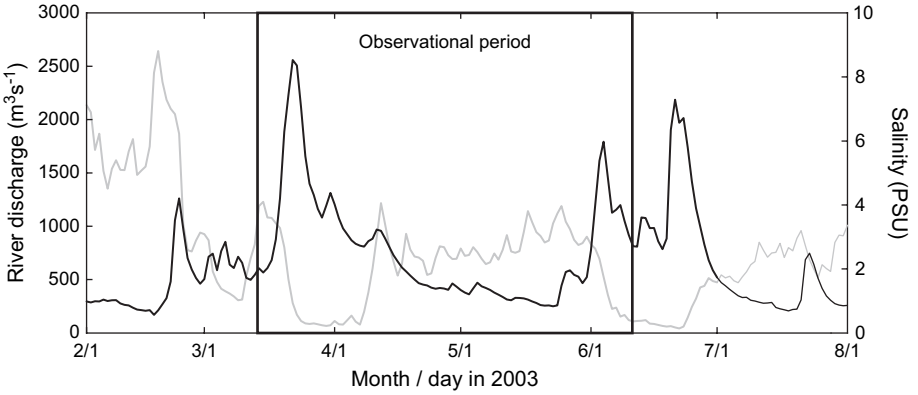

Fig. 3. Combined daily mean discharge of the Delaware, Schuylkill and Christina rivers in Spring 2003 from USGS records (black line). Note that two river peak-flow events occurred during the observational period. Also plotted is a USGS record of surface salinity measured at Reedy Island (gray line).

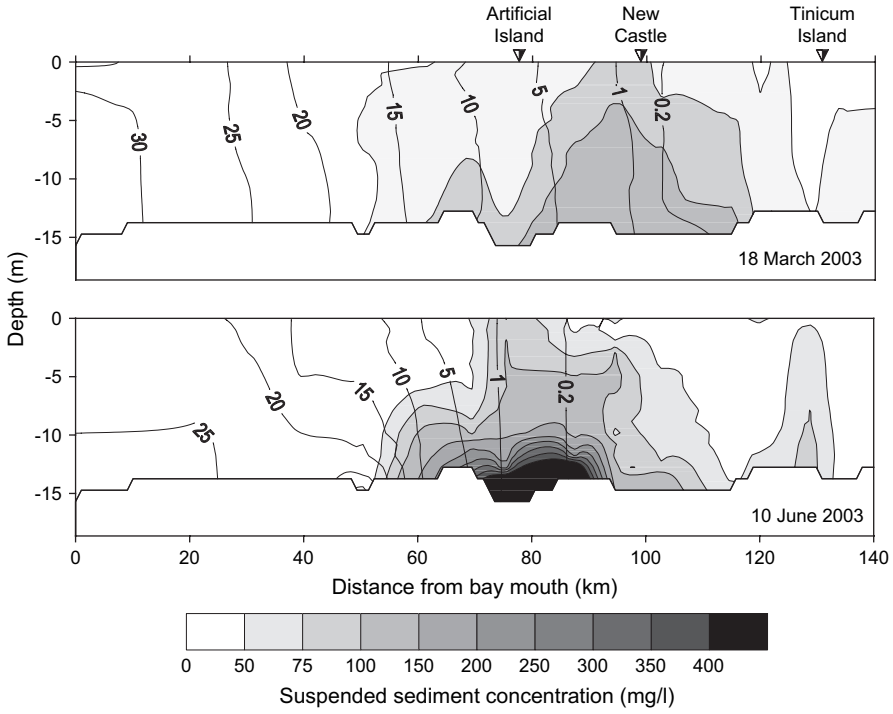

Fig. 4. Axial distributions of salinity and SSC from data collected during surveys on 18 March and 10 June 2003 at the beginning and end of the observational period (see Fig. 3). Note the relative locations of the salt intrusion (0.2 isohaline) and the high-concentration ETM core. See text for description of data.

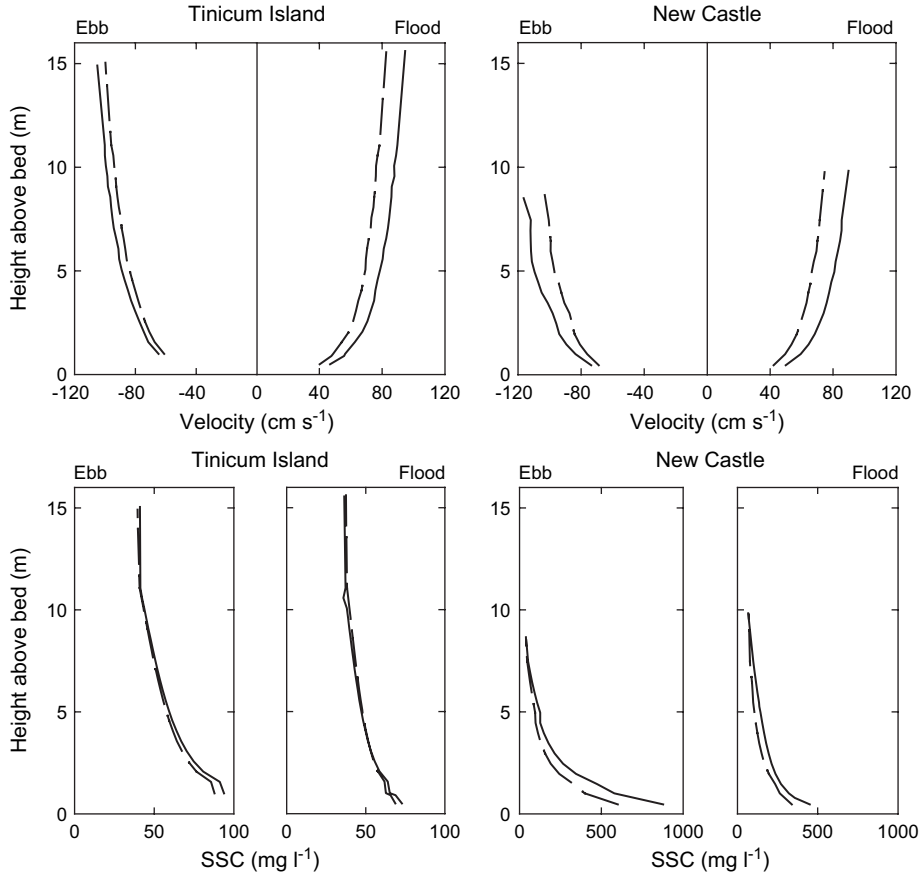

Fig. 5. Profiles of current velocity and modeled SSC concentration at Tinicum Island (left) and New Castle (right) averaged over the 80-day period of observation. Shown are flood-phase (solid line) and ebb-phase (dashed line) averages for all spring and neap tides. See text for description of data.

to the free surface during peak tidal flow (Fig. 5). Current speed within 1 m above the bottom was generally 40–50% lower than at the surface, and the surface speed during spring tides was roughly 150% higher than at neap. Spring–neap variations in current speed and vertical shear were similar at both sites, but flood–ebb variation in speed was greater at New Castle. Modeled profiles of SSC exhibited a similar logarithmic shape at both sites (Fig. 5). Flood–ebb variations in the gradient of SSC profiles were more pronounced than spring–neap variations, and at both sites near-bottom SSC was nearly twofold higher on ebb than on flood due to stronger ebb currents. Depth variation in SSC was larger at New Castle than at Tinicum Island, presumably due to a larger supply of resuspendable sediment. Assuming a quadratic relationship between the critical current velocity (measured by the ADV) and critical shear stress for resuspension, and using total drag coefficients representative for the bottom (0.0022–0.0025; Soulsby, 1983), the resuspension stress at both sites is estimated at 0.1–0.3 N m^{-2}. This stress range is typical for estuarine flocs in general (Whitehouse et al., 2000), but in the present case it is only approximate because form-drag and skin-friction subcomponents of the total drag cannot be separated with the available data. Values of bulk settling velocity (W_s) computed by inverting the Rouse equation averaged 0.40 cm s^{-1} and 0.18 cm s^{-1} at New Castle and Tinicum Island, respectively.

To highlight site-specific relationships between bottom currents and SSC, subsamples of the instantaneous (burst-averaged) ADV and SSC data for spring and neap tides are presented in Figs. 6 and 7. Tidal currents modulated SSC at both locations, but the dependence of SSC on current speed was highly site-specific. At Tinicum Island, a SSC peak typically occurred just before maximum ebb as the current exceeded the critical value for resuspension ($U_{cr} = 30 \pm 7$ cm s^{-1}), and the peak amplitude was higher at spring tides than at neap (Fig. 6). This pattern is consistent with depletion of a local sediment source early in the tidal cycle, i.e., resuspension of flocs that had settled during the previous slackwater period. A broader SSC peak typically occurred after maximum ebb, but not after maximum flood. This implies that ebb-current resuspension and advection yields a net down-estuary flux of suspended sediment at Tinicum Island. Then again, the dependence of SSC on current speed at this site was weak to non-existent due to a general lack of easily resuspendable sediment (Fig. 6). Despite the relatively high bulk W_s value at Tinicum Island (Table 1), tidal resuspension and seaward transport prevents the formation of mud deposits locally.

The influence of tidal currents on SSC was pronounced at the New Castle site due to an abundance of resuspendable sediment within the ETM zone. SSC increased with increasing ebb and flood flow (Fig. 7), peaked at maximal velocity, and did not drop until the current decreased to below the critical speed for resuspension ($U_{cr} = 30 \pm 8$ cm s^{-1}). The amplitude of SSC peaks was higher during ebb than on flood due to stronger ebb currents particularly during spring tides (Fig. 7). During waning flood and ebb flow, small SSC spikes superimposed on the falling limb of the curve may manifest

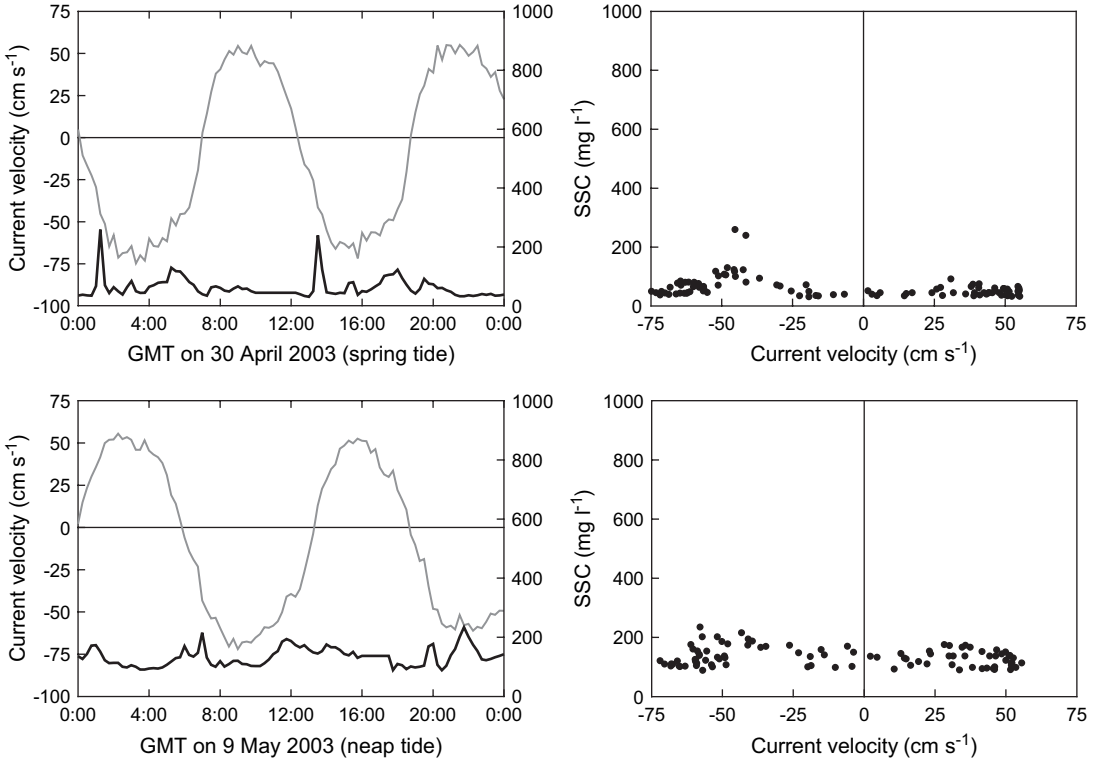

Fig. 6. Subsampled records of current velocity and SSC measured 0.9 and 0.7 m above bottom, respectively, for a spring tide (top left) and neap tide (bottom left) at the Tinicum Island site. Also shown are scatter plots (at right) of the same data. See text for explanation of data.

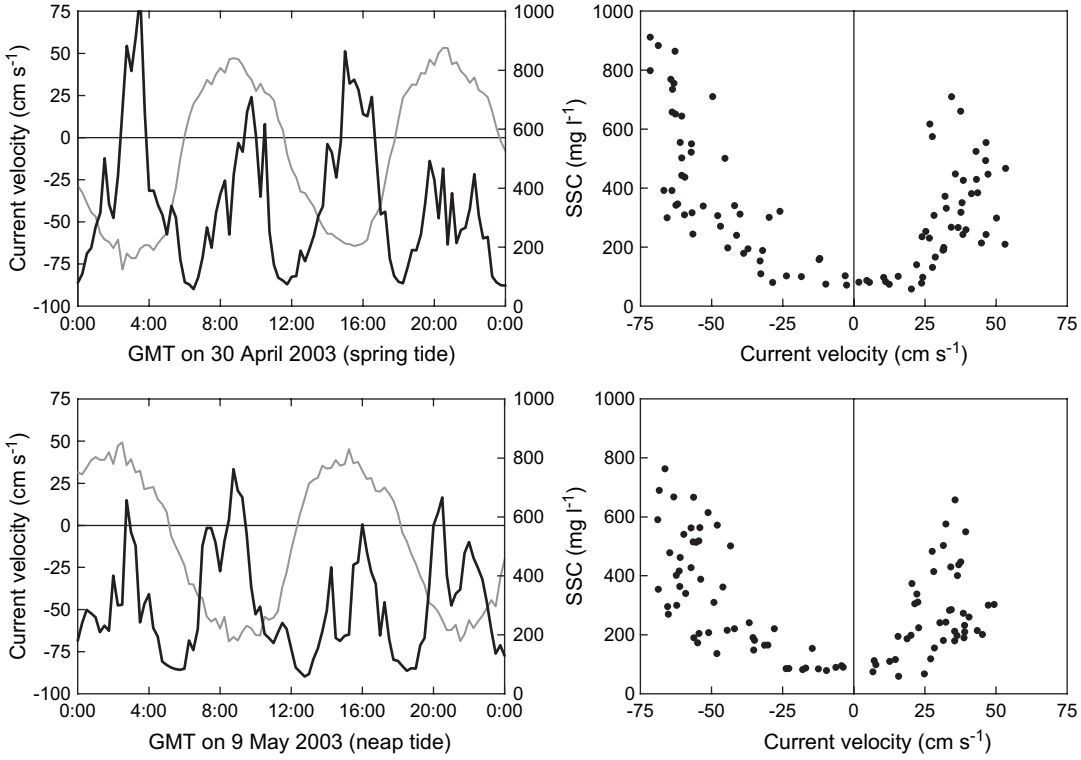

Fig. 7. Subsampled records of current velocity and SSC measured at 0.5 and 0.8 m above bottom, respectively, for a spring tide (top left) and neap tide (bottom left) tide at the New Castle site. Scatter plots are also shown (at right). See text for explanation of data.

sediment advection transverse to the channel axis. In contrast to Tinicum Island, there was no evidence of sediment-source depletion during the tidal cycle at New Castle, presumably due to the proximity of this site to the ETM.

The complete timeseries of instantaneous water depth (h), currents and SSC for the 80-day period of measurement are presented in Fig. 8, and the data are summarized in Table 1. Depth-averaged, along-channel current velocity, $\langle U \rangle$, was computed by integrating the composite velocity profile over h, whereas depth-averaged SSC, $\langle C \rangle$, was calculated in a similar manner from modeled SSC profiles. At both mooring sites $\langle U \rangle$ was strongly ebb-dominant throughout the period of record, and mean values were typically 10–15 cm s^{-1} higher at spring tides than at neap. Maximum mean values of $\langle U \rangle$ during the ebb phase of spring tides were 90 cm s^{-1} and 95 cm s^{-1} at Tinicum and New Castle, respectively. Overall, tidal variations in $\langle C \rangle$ ranged from 20–450 mg L^{-1} at New Castle to 10–130 mg L^{-1} at Tinicum Island.

4.3. Subtidal variation in currents and SSC

Tidal variations in the timeseries of h, $\langle U \rangle$and $\langle C \rangle$were removed using a 36-h Lanczos filter to resolve subtidal variations related to river discharge and wind forcing (Fig. 8). Overall, tidally averaged water depth, $\overline{h}$, depth-averaged velocity, $\langle \overline{U} \rangle$, and depth-averaged SSC, $\langle \overline{C} \rangle$, varied by as much as ± 0.75 m, ± 25 cm s^{-1}, and ± 100 mg L^{-1}, respectively. River discharge was the dominant source of subtidal current variability; cross-correlation analysis suggests a strong negative (seaward) correlation between river discharge and $\langle \overline{U} \rangle$ at New Castle (86%) and Tinicum (96%). Significantly, the freshets in March and June increased $\langle \overline{U} \rangle$ by about a factor of two. The most conspicuous feature of the subtidal record is a seaward Eulerian mean current averaging -13 cm s^{-1} at Tinicum and -16 cm s^{-1} at New Castle (negative values denote ebb or seaward flow). This non-tidal drift is primarily compensatory flow for Stokes drift on flood (e.g., Uncles and Jordan, 1979), and in the upper Delaware Estuary arises from non-zero correlations between tidal height and current. The average contribution of river discharge to the non-tidal drift is estimated at $\sim$4 cm s^{-1} based on gauged river discharge during the study period.

Despite the clear influence of river discharge on subtidal flow, the freshets had contrasting affects on SSC variability at the measurement sites. At Tinicum Island, little to no change in $\langle \overline{C} \rangle$ was apparent during the March or June freshet events (Fig. 8); either the amount of sediment remobilized by the intensified bottom currents was insignificant, or the suspended material bypassed the mooring undetected. During the first 2 months of observation, $\langle \overline{C} \rangle$ gradually increased and peaked in mid-May as sediment resuspended by the March freshet transited the tidal river. At New Castle, $\langle \overline{C} \rangle$ initially increased with rising river discharge and $\langle \overline{U} \rangle$ during the March freshet, but then it decreased before peak riverflow (compare Figs. 3 and 8). This response is intuitive given the proximity of New Castle to the ETM—elevated riverflow should displace the ETM seaward and temporarily decrease $\langle \overline{C} \rangle$ in the upper estuary. In contrast, because Tinicum Island falls far landward of the ETM, $\langle \overline{C} \rangle$ should vary with sediment delivery from the tidal river.

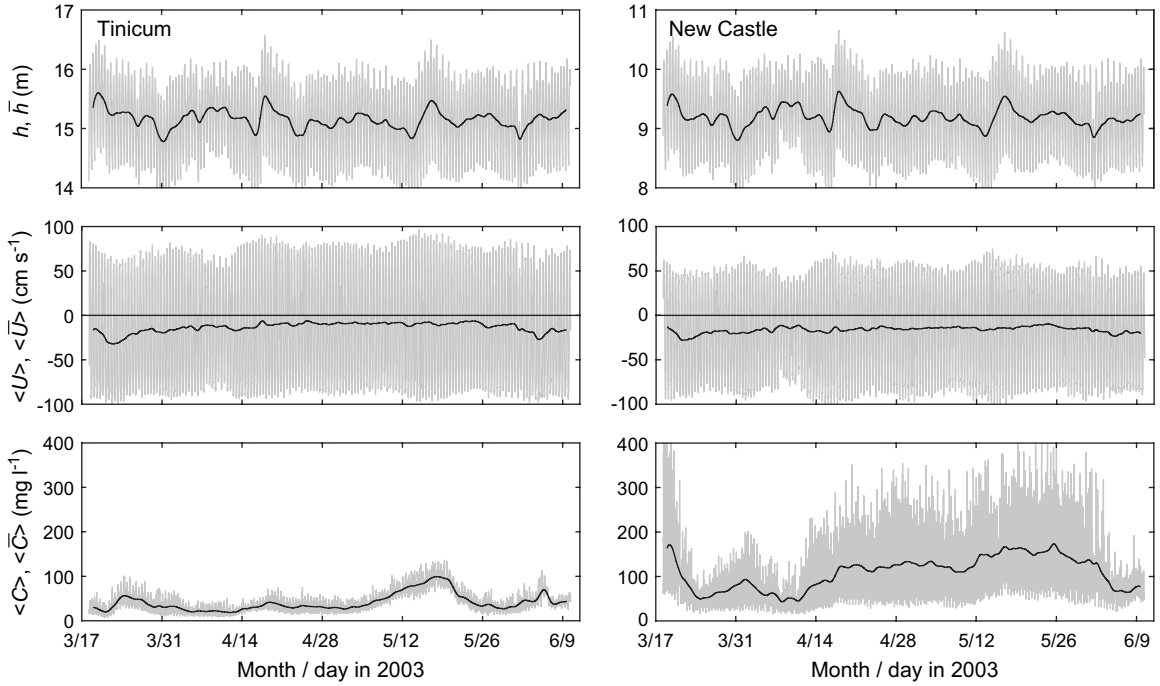

Fig. 8. Records of tidal and residual (tide filtered) water level (h, $\overline{h}$), depth-averaged tidal and residual current velocity($\langle U\rangle$, $\langle\overline{U}\rangle$), and depth-averaged tidal and residual SSC ($\langle C\rangle$, $\langle\overline{C}\rangle$) for the observational period. Bold lines are low-pass filtered data. See text for description of data.

To examine the extent of remote-wind effects on subtidal variability in upper estuary, hourly wind velocity data from NDBC Station 44009 were interpolated at 15 min intervals, decomposed into 10° increments relative to North (negative velocities representing 180° to 350°), and low-pass filtered. Cross-correlation coefficients were calculated between time series data and each of the wind velocity subrecords. The direction of strongest correlation between wind speed and water level in the upper estuary was 50° (along-shelf at the bay mouth), and the filtered record of this subcomponent is shown in Fig. 9. Three northeasterly wind events of magnitude $\geq$10 m s^{-1} occurred during the study period, two of which (17 April and 17 May) increased $\overline{h}$ by nearly 100 cm and decreased $\langle\overline{U}\rangle$ by $\sim$5 cm s^{-1} at both sites (compare Figs. 8 and 9). The influence of remote winds decreased up-estuary; cross correlation of 50° winds and $\overline{h}$ indicates a 74% correlation at New Castle and a 65% correlation at Tinicum (the correlation between wind and sea level is actually higher when the time lag between the two is taken into consideration). Coastal winds at 50° and $\langle\overline{U}\rangle$ at New Castle were correlated at 39%, whereas the correlation at Tinicum was lower at 25%.

4.4. Sectionally averaged flux and error analysis

Cross-sectionally averaged tidal fluxes of water and suspended sediment were computed to estimate cumulative mass transport through the upper estuary during the observational period. Here we emphasize that because currents and SSC were sampled at only one station per section, the reported fluxes are speculative (but reasonable) estimates. Tidal variations in total water discharge (Q) were determined from the rate of change of tidal height and estuarine surface area, assuming continuity. This technique, which reduces uncertainties associated with lateral extrapolation of current-meter data, is applicable in the study given the lack of density-driven flow. The upper estuary was divided into two segments: (1) Trenton to Tinicum Island; and (2) Tinicum Island to New Castle. Values of Q at the lower end of each segment were computed from

$$Q(t) = A_s(t)\frac{\partial\eta}{\partial t} \quad (1)$$

where A_s is the surface area of the segment and η is the free-surface elevation. Surface area was determined using a Geographical Information System (GIS), and water elevation was determined from the timeseries of tidal height. The timeseries of Q was then low-pass filtered to derive residual discharge ($\overline{Q}$), which approximates total riverflow entering the

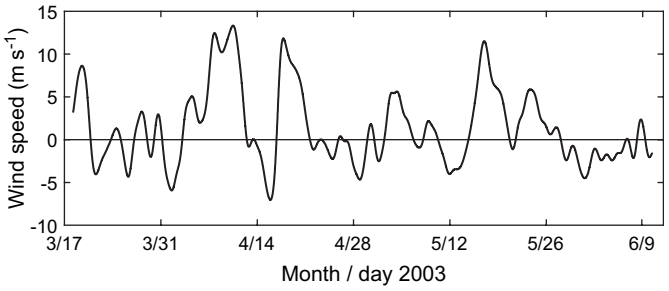

Fig. 9. Record of wind speed (50° from North) at NDBC Buoy 44009 for the study period (see Fig. 1 for location). Major wind events ($\geq$5 m s^{-1}) correlated with increases in subtidal water level (Fig. 8) and decreases in subtidal discharge (Fig. 10) in the upper estuary.

upper estuary at Tinicum Island. Finally, timeseries of tidal and residual sediment flux were computed as the product of Q and $\langle C \rangle$ and $\overline{Q}$ and $\langle \overline{C} \rangle$, respectively, where $\langle C \rangle$ is the depth-averaged concentration as described earlier.

An error budget was developed to provide limits of uncertainty for the estimated sediment fluxes. The three chief sources of quantifiable error were as follows: (1) tidal discharge error (Q estimated from eq. (1)); (2) calibration of OBS sensors; and (3) lateral extrapolation of $\langle C \rangle$ over cross-sectional area. First, independent measurements of Q in the upper Delaware Estuary made through shipboard ADCP surveys (Sommerfield et al., 2006) indicate that eq. (1) is accurate to within 2% of measured discharge. This level of agreement is expected given the simple geometry of the estuarine channel. Second, the uncertainty associated with the calibration of OBS-3 sensors is ±5% of computed SSC based on the standard error of regression parameters. Lastly, and by far the largest source of uncertainty (20–30%), is related to sectional extrapolation of $\langle C \rangle$. This error was estimated following a method adapted from Wall et al. (2006) in which depth-averaged SSC at a single station is regressed against synoptic cross-sectional averages. In the present case, station and sectionally averaged data were obtained during the aforementioned ADCP surveys using a combination of shipboard and moored measurements of SSC and currents (Sommerfield et al., 2006). In total, the confidence limits of sectionally averaged sediment fluxes computed for this study are 27–37%.

Records of tidal and residual (tide filtered) discharge and sediment flux are shown in Fig. 10. Tidal discharge varied largely with spring–neap cyclicity; maximum discharge during spring tides averaged 12,000 $m^3\ s^{-1}$ at Tinicum Island and 15,000 $m^3\ s^{-1}$ at New Castle, whereas neap tide discharges were 8000 $m^3\ s^{-1}$ and 10,000 $m^3\ s^{-1}$, respectively. Maximum seaward residual discharge was associated with river peakflows, and periods of landward residual flow coincided with remote-wind events on 17 April and 17 May (compare Figs. 9 and 10). Tidal sediment flux ranged from −100 to −1500 kg s^{-1} at Tinicum Island and from −500 to −5000 kg s^{-1} at New Castle (Fig. 10). Residual sediment flux was seaward at both sites throughout the study period, ranging from −20 to −120 kg s^{-1} at Tinicum Island and from −100 to −470 kg s^{-1} at New Castle. Maximum and minimum residual sediment fluxes coincided with freshet and remote-wind events, respectively. Integrated over the 80-day study period, the cumulative residual sediment flux past New Castle ($11 \pm 4 \times 10^8$ kg) was significantly larger than at Tinicum Island ($4 \pm 1 \times 10^8$ kg) at the maximum level of uncertainty (Fig. 11). The Christina River, the only intervening tributary of significance, delivered an estimated 6.0×10^7 kg of suspended sediment during the study period, insufficient to balance the difference between the sectional fluxes. The most probable explanation for this difference is that bottom erosion *within* the study segment contributed a large quantity ($\sim 7 \times 10^8$ kg) of the sediment exported to the lower estuary.

5. Discussion

5.1. Net sediment flux in river estuaries

The movement of fine-grained sediment from non-tidal river reaches to estuaries is a discontinuous process characterized by punctuated transport, storage, and remobilization. Upon reaching the estuary, processes indigenous to the ETM zone modulate the dispersal of sediment to burial sites. Although the along-estuary position of the ETM varies with a number of factors, excursions forced by river discharge is the most universal observation (e.g., Allen et al., 1980; Schubel and Pritchard, 1986; Uncles et al., 1994; Grabemann et al., 1997; Geyer et al., 2001; Sanford et al., 2001). In general, the Delaware Estuary salt front generally shifts ~4 km seaward for every 340 $m^3\ s^{-1}$ increase in freshwater discharge

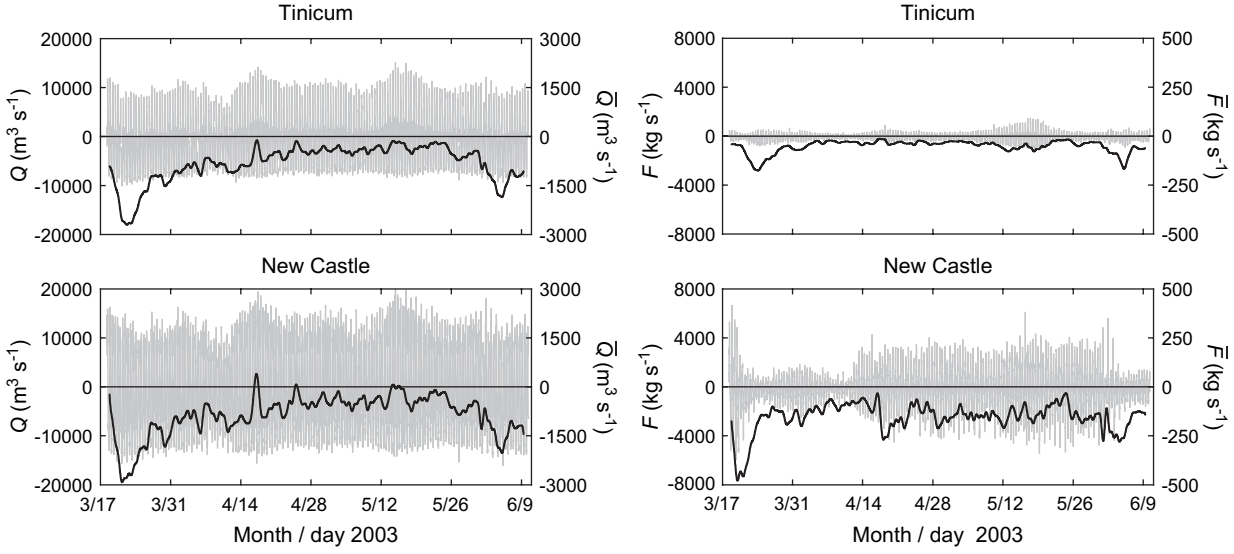

Fig. 10. Sectionally averaged tidal and residual discharge (Q, $\overline{Q}$) and sediment flux (F, $\overline{F}$) at the Tinicum Island and New Castle sites. Note that the low-passed data shown by the bold line are plotted on a different scale to highlight the subtidal variability. See text for description of data.

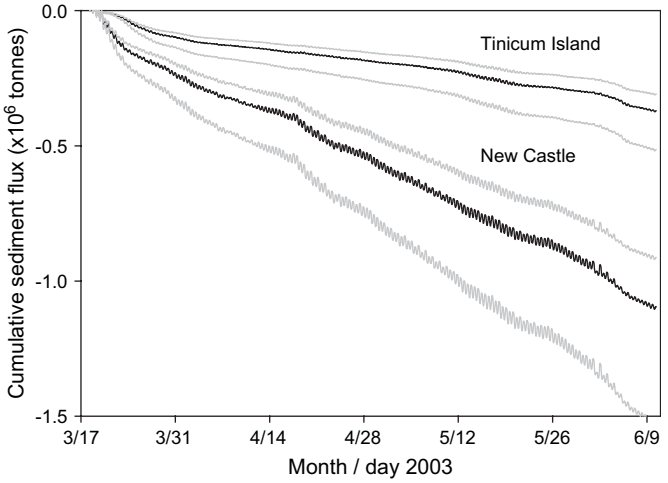

Fig. 11. Records of cumulative sediment flux past Tinicum Island and New Castle during the observational period. Negative values denote seaward net fluxes, and the gray lines represent the maximum 37% level of uncertainty. The larger cumulative flux past New Castle suggests that bottom erosion in the upper estuary sourced a significant amount of the sediment exported to the lower estuary.

(Garvine et al., 1992). Accordingly, the observed 1200 $m^3\ s^{-1}$ increase in riverflow can explain why the salt front and ETM zone in June were displaced seaward of their locations in March, and also why the water column was more stratified. This is supported by the SSC timeseries at New Castle, i.e., decreasing concentrations at peak riverflow with seaward displacement of the ETM (Fig. 8). The subsequent increase in SSC from mid-April to early June is consistent with decreasing riverflow and the return of ETM sediment via tidal pumping, though some of this increase is likely related to sediment delivered from up-estuary sources.

Although wind forcing was found to be subordinate to river discharge in controlling the subtidal sediment flux, it is worth discussing the role of wind-induced transport in the upper estuary. The most conspicuous wind effect was associated with the remote wind field, namely, sea-level setup in the estuary and reduced seaward residual flow. The narrow width of the upper estuary along with changes in channel direction limit the local wind fetch such that wave-orbital is insufficient to resuspend channel-floor sediments. The situation is quite different in Delaware Bay, where local wind stress imparts a significant influence on subtidal variability than remote winds and coastal setup (Janzen and Wong, 2002). North et al. (2004) modeled wind forcing of the ETM in the Chesapeake Bay and found down-estuary wind stress resulted in up-estuary movement of the salt front and suspended-sediment concentration. This is consistent with observations of a baroclinic response to wind forcing that enhances landward and seaward flow in bottom and surface waters, respectively (Wang, 1978). Such an effect is less likely to occur in the well-mixed upper Delaware Estuary due to a small wind fetch, and also because landward gravitational circulation is weak to non-existent compared to the partially stratified lower estuary and bay.

5.2. Intra-estuary sediment storage

In addition to delivering new sediment from the non-tidal river, our results reveal that typical freshet peakflows (1000–2000 $m^3\ s^{-1}$) remobilize fine-grained deposits stored within the upper estuary. Evidence for such an effect is twofold. First, the secondary ETM observed in June 2003 (Fig. 3) manifests a pool of easily resuspendable sediment that does not appear to exchange with the primary ETM on a tidal time scale. In 2003, this localized source was likely mud trapped in the axial shipping channel (Fig. 1). If not first removed by dredging, such material could move down-estuary upon being eroded by freshet-enhanced tidal currents. Second, the mass of internally produced sediment ($7 \pm 2 \times 10^8$ kg) exceeded the total load of sediment ($5 \pm 1 \times 10^8$ kg) delivered by the three main tributaries (Delaware, Schuylkill, and Christina rivers). Hence, even if the cumulative sediment flux at Tinicum ($4 \pm 1 \times 10^8$ kg) was underestimated due to the off-channel location of the measurement site, a significant intra-estuary source of sediment is evidenced by the difference between tributary and New Castle fluxes. Because these observations were made during typical springtime freshet flows, it is reasonable to conclude that net export of sediment from the upper to lower estuary under such flows is a general characteristic of the system.

Further generalization of the sedimentary system is problematic given the number of factors that influence circulation, SSC and sediment storage in the Delaware Estuary. Indeed, recall that on two occasions the seaward residual sediment flux came close to reversing direction on account of remote-wind forcing; strong winds in conjunction with low riverflow may have been sufficient to generate an up-estuary sediment flux. Perhaps most vexing is the effect of sediment storage on tidal and seasonal sediment fluxes, as this is dependant on conditions from previous years. Quantifying inter-annual storage would require either multiyear observations of sediment flux or bed volume (e.g., Bale et al., 1985), but unfortunately both approaches are difficult to carry out in estuaries at the appropriate measurement density. A further complication is maintenance dredging in the upper Delaware Estuary, which has a direct bearing on the mass of sediment released from storage during peakflows. For example, the shipping channel had not been dredged for at least one year prior to Spring 2003—spot sampling revealed it to be filled with high-porosity mud. Had this study been conducted immediately following a dredging campaign it is likely that the measured cumulative flux would have been smaller.

It remains to explain how sediment becomes sequestered in the upper estuary in the first place, a question that without direct observations can only be speculated. One possibility is that sediment transported down-estuary early in the year returns via tidal pumping in late summer when the seaward non-tidal drift is relatively weak. This form of sediment recirculation is independent of the landward gravitational circulation and has been documented in river estuaries worldwide (e.g., Allen et al., 1980; Geyer et al., 2001). During periods of low river discharge, up-estuary mass fluxes can be generated

by bottom erosion triggered by spring tidal currents (Bale et al., 1985; Woodruff et al., 2001). The large *tidal* sediment fluxes observed in the present study suggest that landward mass transport and trapping is certainly possible even though a landward *residual* flux was not measured. If so, then it is possible that some of the sediment transported to the lower Delaware Estuary in Spring 2003 was sequestered in the upper estuary during a previous year. The mechanisms and seasonality of this pathway are currently under investigation, but the fact that more sediment is dredged from the upper Delaware Estuary on average than is supplied by rivers suggests that much of the dredged material originates from erosional sources in the lower estuary (USACE, 1973; Walsh, 2004).

6. Summary and conclusions

(1) In Spring 2003, the Delaware Estuary turbidity maximum migrated axially in association with river peakflows of 1000–2000 $m^3\ s^{-1}$, typical springtime events with a recurrence interval of 1–2 years. Such flows are capable of displacing the salinity intrusion and suspended sediment trapped within the ETM zone ~20 km to seaward, while at the same time increasing salinity stratification and suspended-sediment mass in the lower estuary. River-forced excursions of the ETM temporarily decrease SSC in the upper estuary, because pools of easily resuspendable sediment are advected seaward.

(2) Spatial and temporal variation in SSC and flux in the upper Delaware Estuary is highly dependent on the proximity of resuspendable bed deposits, some of which reside in quasi-stationary depositional zones. At both measurement sites the critical velocity for resuspension within 1 m above the bottom was $30 \pm 8\ cm\ s^{-1}$ (0.1–0.3 $N\ m^{-2}$ estimated bed stress). SSC was not correlated with tidal current velocity at Tinicum Island (silty sand bottom) due to rapid depletion of local bed-sediment sources early in the tidal cycle. In contrast, SSC and currents at New Castle (muddy bottom) were well correlated due to an abundance of resuspendable sediment available in the ETM zone. Throughout the study period the depth-averaged residual current and sediment flux were seaward, and the flux magnitude increased 3–4 fold during river peakflows on account of elevated ebb currents and bottom scour. The seaward residual current that occurs in compensation for Stokes Drift on flood tide appears to be a significant mechanism of sediment transport to the estuarine turbidity maximum zone.

(3) Although subtidal variations of currents and SSC in the upper Delaware Estuary are forced principally by freshwater discharge, remote winds during the study period had a measurable influence on residual flow. Sustained along-shelf winds (50° from North) of speeds $\geq 10\ m\ s^{-1}$ increased water levels in the upper estuary by nearly 100 cm and reduced the non-tidal drift by $\sim 5\ cm\ s^{-1}$. Remote-wind forcing and estuarine setup had a much smaller influence on residual sediment flux during the study period, but this effect could be more significant given the appropriate environmental conditions.

(4) Sediment mass balance suggests that the upper estuary channel is a quantitatively important repository of sediment on inter-annual timescales. During the 80-day observational period, the estimated sediment load delivered by tributaries to the study area was $5 \pm 1 \times 10^8$ kg. By comparison, the sectionally averaged sediment flux at Tinicum Island (landward end) was $4 \pm 1 \times 10^8$ kg, whereas $11 \pm 4 \times 10^8$ kg was measured at New Castle (seaward end). The flux imbalance ($\sim 7 \times 10^8$ kg) implies that deposits remobilized from storage within the intervening channel were a significant source of sediment delivered to the lower estuary. In view of these results, and given the persistence of sediment deposition in the upper estuary (as evinced by dredging records), we speculate that suspended sediment becomes entrapped by up-estuary tidal pumping and deposition during periods of low riverflow.

Acknowledgments

We would like to thank the capable crew of the RV *Cape Henlopen* and A. Sundberg for assistance with the hydrographic surveys and mooring operations. David Walsh and Elyse Scileppi provided valuable technical assistance shipboard and in the laboratory. We also thank Larry Sanford for his thoughtful comments on an early draft of the manuscript, and two anonymous reviewers for constructive insights. This research was supported by Delaware Sea Grant award SG R/ME-35 to C.S. and K.C.W. Additional support was provided by a Sigma Xi Grant-in-Aid of Research to T.C.

References

Allen, G.P., Salomon, J.C., Bassoullet, P., Du Penhoat, Y., De Grandpre, C., 1980. Effects of tides on mixing and suspended sediment transport in macrotidal estuaries. Sedimentary Geology 26, 69–90.

Bale, A.J., Morris, A.W., Howland, R.J.M., 1985. Seasonal sediment movement in the Tamar estuary. Oceanologica Acta 8, 1–7.

Biggs, R.B., Beasley, E.L., 1988. Bottom and suspended sediments in the Delaware River and Estuary. In: Majumdar, S.K., Miller, E.W., Sage, L.E. (Eds.), Ecology and Restoration of the Delaware River Basin. The Pennsylvania Academy of Science, pp. 116–131.

Biggs, R.B., Sharp, J.H., Church, T.M., Tramontano, J.M., 1983. Optical properties, suspended sediments, and chemistry associated with the turbidity maxima of the Delaware Estuary. Canadian Journal of Fisheries and Aquatic Science 40 (Supplement 1), 172–179.

Cook, T.L., 2004. Observations of Sediment Transport in the Delaware Estuary During Spring Runoff Conditions. Unpublished M.S. thesis, University of Delaware, Newark, 64 pp.

Galperin, B., Mellor, G.L., 1990. A Time-dependant, three-dimensional model of the Delaware Bay and River system. Part 1: description of the model and tidal analysis. Estuarine, Coastal and Shelf Science 31, 231–253.

Garvine, R.W., McCarthy, R.K., Wong, K.-C., 1992. The axial salinity distribution in the Delaware Estuary and its weak response to river discharge. Estuarine, Coastal and Shelf Science 35, 157–165.

Geyer, W.R., Woodruff, J.D., Traykovski, P., 2001. Sediment transport and trapping in the Hudson River Estuary. Estuaries 24, 670–679.

Gibbs, R.J., Konwar, L., Terchunian, A., 1983. Size of flocs suspended in Delaware Bay. Canadian Journal of Fisheries and Aquatic Sciences 40 (Suppl. 1), 102–104.

Grabemann, I., Uncles, R.J., Krause, G., Stephens, J.A., 1997. Behavior of turbidity maxima in the Tamar (U.K.) and Weser (F.R.G.) estuaries. Estuarine, Coastal and Shelf Science 45, 235–246.

Janzen, C.D., Wong, K.-C., 2002. Wind-forced dynamics at the estuary-shelf interface of a large coastal plain estuary. Journal of Geophysical Research 107, 3138–3139.

Kearney, M.S., Rogers, A.S., Townshend, J.R.G., Rizzo, E., Stutzer, D., Stevenson, J.C., Sundborg, K., 2002. Landsat imagery shows decline of coastal marshes in Chesapeake and Delaware Bays. Eos, Transactions of the American Geophysical Union 83, 173.

Kineke, G.C., Sternberg, R.W., 1992. Measurement of high concentration suspended sediments using the optical backscatterance sensor. Marine Geology 108, 253–258.

Kraft, J.C., Yi, H., Khalequzzaman, M., 1992. Geologic and human factors in the decline of the salt marsh lithosome: the Delaware Estuary and Atlantic coastal zone. Sedimentary Geology 80, 233–246.

Mansue, L.J., Commings, A.B., 1974. Sediment transport by streams draining into the Delaware Estuary. U.S. Geological Survey Water Supply Paper 1532-H. U.S. Geological Survey, Washington, 17 pp.

Münchow, A., Masse, A.K., Garvine, R.W., 1992. Astronomical and nonlinear tidal currents in coupled estuary shelf system. Continental Shelf Research 12, 471–498.

North, E.W., Chao, S.-Y., Sanford, L.P., Hood, R.R., 2004. The influence of wind and river pulses on an estuarine turbidity maximum: numerical studies and field observations in Chesapeake Bay. Estuaries 37, 132–146.

Orton, P.M., Kineke, G.C., 2001. Comparing calculated and observed vertical suspended-sediment distributions from a Hudson River Estuary turbidity maximum. Estuarine, Coastal and Shelf Science 52, 401–410.

Pape III, E.H., Garvine, R.W., 1982. The subtidal circulation in Delaware Bay and adjacent shelf waters. Journal of Geophysical Research 87, 7955–7970.

Parker, B.B., 1991. The relative importance of the various nonlinear mechanisms in a wide range of tidal interactions (review). In: Parker, B.B. (Ed.), Tidal Hydrodynamics. John Wiley and Sons, New York, pp. 237–268.

Sanford, L.P., Suttles, S.E., Halka, J.P., 2001. Reconsidering the physics of the Chesapeake Bay estuarine turbidity maximum. Estuaries 24, 655–669.

Schubel, J.R., Pritchard, D.W., 1986. Responses of the upper Chesapeake Bay to variations in discharge of the Susquehanna River. Estuaries 9, 236–249.

Sharp, J.H., Cifuentes, L.A., Coffin, R.B., Pennock, J.R., Wong, K.-C., 1986. The influence of river variability on the circulation, chemistry and microbiology of the Delaware Estuary. Estuaries 9, 261–269.

Sommerfield, C.K., Madsen, J.A., 2004. Sedimentological and Geophysical Survey of the Upper Delaware Estuary. University of Delaware Sea Grant Publication DEL-SG-04-04, 126 pp.

Sommerfield, C.K., Wong, K.-C., Yang, H., 2006. Morphologic control of residual sediment flux in the Delaware River Estuary. Annual meeting of the Geological Society of America, Abstracts with Programs, p. 185.

Soulsby, R.L., 1983. The bottom boundary layer of shelf seas. In: Johns, B. (Ed.), Physical Oceanography of Coastal and Shelf Seas. Elsevier Oceanography Series 35, pp. 189–266.

Syvitski, J.P., Morehead, M.D., Bahr, D.B., Mulder, T., 2000. Estimating fluvial sediment transport: The rating parameters. Water Resources Research 36, 2747–2760.

Uncles, R.J., Jordan, M.B., 1979. Residual fluxes of water and salt at two stations in the Severn Estuary. Estuarine and Coastal Marine Science 9, 287–302.

Uncles, R.J., Barton, M.L., Stephens, J.A., 1994. Seasonal variability of fine-sediment concentrations in the turbidity maximum region of the Tamar Estuary. Estuarine, Coastal and Shelf Science 38, 19–39.

U.S. Army Corps of Engineers, 1973. Long Range Spoil Study, Part III, Sub-Study 2. Nature, Source, and Cause of Shoal. U.S. Army Engineering District, Philadelphia Corps of Engineers, North Atlantic Division, Philadelphia, Pennsylvania, 95 pp.

U.S. Geological Survey, 2005. USGS Suspended-sediment Database, Daily Values of Suspended Sediment and Ancillary Data. http://co.water.usgs.gov/sediment/seddatabase.cfm.

Wall, G.R., Nystrom, E.A., Litten, S., 2006. Use of an ADCP to compute suspended-sediment discharge in the tidal Hudson River, New York. U.S. Geological Survey Scientific Investigations Report 2006-5055, 16 pp.

Walsh, D.R., 2004. Anthropogenic influences on the morphology of the tidal Delaware River and Estuary: 1877–1987. Unpublished M.S. thesis, University of Delaware, Newark, Delaware, 90 pp.

Wang, D.-P., 1978. Wind-driven circulation in the Chesapeake Bay, Winter 1975. Journal of Physical Oceanography 9, 564–572.

Whitehouse, R.J.S., Soulsby, R.L., Roberts, W., Mitchener, H.J., 2000. Dynamics of Estuarine Muds. Thomas Telford, London, 210 pp.

Wong, K.-C., Moses-Hall, J.E., 1998. The tidal and subtidal variations in the transverse salinity and current distributions across a coastal plain estuary. Journal of Marine Research 56, 489–517.

Wong, K.-C., Garvine, R.W., 1984. Observations of wind-induced, subtidal variability in the Delaware Estuary. Journal of Geophysical Research 89, 10589–10597.

Woodruff, J.D., Geyer, W.R., Sommerfield, C.K., Driscoll, N.W., 2001. Seasonal variation of sediment deposition in the Hudson River estuary. Marine Geology 179, 105–119.